Significant enhancement of high-order harmonics below 10 nm in a two-color laser field

T. T. Liu, T. Kanai, T. Sekikawa,* and S. Watanabe
Institute for Solid State Physics, University of Tokyo, 5-1-5 Kashiwanoha, Kashiwa 277-8581, Japan
(Received 6 February 2006; published 23 June 2006)

Efficient high-order harmonic generation was obtained in helium below 10 nm using a linearly polarized two-color field consisting of a Ti:sapphire laser pulse (ω) with a 40-fs duration and its second harmonic (2ω) with a 24-fs duration. The intensity of the two-color harmonics was enhanced more than that of the ω or 2ω field alone by more than one order of magnitude along with the extension of the cutoff order and the generation of efficient even-order harmonics. This observation was explained by the contribution of the lower branch rather than the upper branch of the cutoff energy, which are split in the ω-2ω field. The supercontinuum around 10 nm provides the bandwidth capable of attosecond pulse generation.

DOI: 10.1103/PhysRevA.73.063823 PACS number(s): 42.65.Ky, 42.50.Hz, 32.80.Rm

I. INTRODUCTION

In the past decades, high-order harmonic generation (HHG) by intense short laser pulses in rare gases has been an attractive target for the potential applications of high-brightness, short-pulse coherent sources in the extreme ultraviolet (XUV) and soft x-ray regions. Considerable efforts have been made experimentally and theoretically to improve the conversion efficiency and to shorten the wavelength of harmonic radiation [1,2]. Among them, the application of a two-color laser field is becoming an attractive research area since the enhancement of harmonic generation by orders of magnitude were observed compared to that generated in the fundamental laser field alone [3–5]. This observation can be easily expected based on the three-step model [6] and is actually supported by numerical calculations [4,5,7].

According to the three-step model, the electron first tunnels from the atomic ground state through the Coulomb barrier by the laser field, and propagates in the external field. Depending on its time of ionization, the electron may return to the atomic core and thereby releases a photon with the energy corresponding to the kinetic energy of the electron plus the ionization potential. The return kinetic energy varies depending on the trajectory the electron follows in the continuum. Based on the three-step model, by varying the frequencies, the polarizations, the relative phase, and the intensities of two ultrashort driving fields, one can in principle manipulate the electron motion in the continuum, and then the harmonic generation.

The enhancement of harmonic intensity is the straight result of the three-step model because the peak instantaneous field is enhanced by the addition of two fields. The even harmonics are simply explained by the breaking of symmetry in the field of the fundamental and its second harmonic (ω-2ω). More recently, modulation in harmonics was demonstrated by controlling the relative phase of two-color fields [8]. Polarization dependences of harmonic generation in the two-color field were investigated [5,9,10]. The generation of circularly polarized high-order harmonic is proposed by the circularly polarized two-color field [9,11,12]. However, the extension of harmonic cutoff frequency and the enhancement of conversion efficiency below 17 nm had never been reported experimentally. The question still remains: where is the cutoff of the enhanced harmonics?

The purposes of this paper are, first, to make an effort to extend the cutoff of the efficient two-color harmonics to the region of the water window (2.3 nm to 4.4 nm) [1,2]; second, to generate intense continuum below 10 nm to cover the bandwidth capable of attosecond pulses [13,14].

The paper is organized as follows: Sec. II describes the experimental apparatus and method. In Sec. III, we present the main results of two-color harmonic generation in neon and helium, which consist of the harmonic generation at different intensities and the polarization-dependent spectra. The analysis of the results is given in Sec. IV. The conditions for the generation of intense higher harmonics in two-color field are discussed in Sec. V. Finally, we summarize in Sec. VI.

II. EXPERIMENTAL SETUP

The experimental setup is schematically shown in Fig. 1. A 10-Hz, 22-fs, 22-TW Ti:sapphire laser system based on chirped pulse amplification was used to generate the fundamental beam [15]. In this experiment, the pulse width was typically 40 fs at 800 nm. The laser power was adjusted by

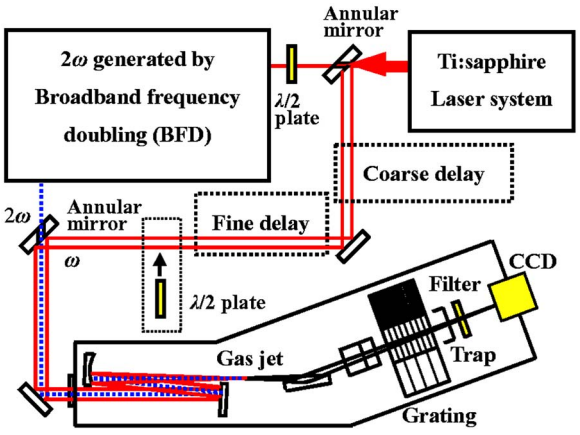

FIG. 1. (Color online) Experimental setup (top view).

*Present address: Department of Applied Physics, Hokkaido University, Kita-13, Nishi-8, Kita-ku, Sapporo 060-8628, Japan.

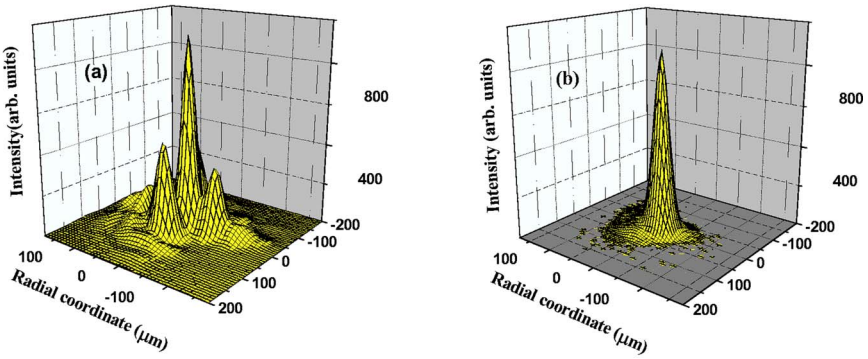

FIG. 2. (Color online) Radial intensity profiles of a Bessel-Gauss beam (a) and a Gauss beam (b) measured in the focal plane using a CCD with a telescope. The Bessel-Gauss beam was generated by the focusing of an annular ω beam (800 nm, $d_{inner}=12$ mm, $d_{outer}=18$ mm) [17], while the Gauss beam came from the circular 2ω beam (400 nm, $d=12$ mm). The corresponding confocal parameters were longer than 14 mm for the two color beams.

changing the pump power or Q-switch timing of the Nd:YAG laser used for a final amplifier. In order to avoid dispersion owing to beam splitters, a mirror with a 12-mm-diameter hole at 45° was used to separate the linearly polarized fundamental laser output into two beams with almost equal intensities. The outer annular beam is sent through a coarse delay line, which compensate for the optical path of broadband frequency doubling, and a fine delay line to shear the ω and 2ω pulses in time. The center circular beam is sent to a broadband frequency doubling (BFD) system to generate the second harmonic (2ω) [16]. BFD enables us to convert a whole spectral component of the fundamental to the second harmonic (SH), resulting in the frequency width of SH wider than that of the fundamental and then the shorter pulse width. The first half of the BFD system consists of a grating (150 line/mm), a two-mirror telescope with a magnification of 0.2 and a 300-μm thick beta-barium borate (BBO) in the middle. The latter half is symmetric to the first half except for a groove density of the grating (300 line/mm). A pulse width of 24 fs was observed by self-diffraction frequency-resolved optical gating (FROG) when the pulse width of the fundamental was 40 fs. The throughput of the BFD system was about 14%.

The polarization of the 2ω pulse was changed to be parallel with that of ω by inserting a half-wave plate for 800 nm (thin mica plate) before BFD. In the experiment of polarization dependence, another half-wave plate was inserted in the path of the ω beam. The two beams were combined coaxially by another mirror with a 12-mm-diameter hole before they entered into a vacuum chamber. Then they were focused by a 50-cm or 100-cm focal-length concave mirror. The 1-mm-diameter nozzle of a pulsed gas jet, which was driven magnetically, was placed 2 to 3 mm behind the superposed focal spots in order to generate harmonics efficiently.

The intensity profiles of the ω and 2ω beams at the focus were enlarged by a telescope and measured by a charge-coupled device (CCD) as shown in Fig. 2. The 2ω beam is well approximated to the Gauss beam and the spot size was 43 μm at full width half maximum (FWHM), corresponding to $M^2=1.7$. The confocal parameter was 14 mm when the 100-cm focal-length mirror was used. On the other hand, the annular ω beam is near to a Bessel-Gauss beam [17] with a central peak accompanied by annular rings at the focus. The spot size of the central peak was 42 μm with the outer diameter (d_{outer}) of 18 mm and the inner diameter (d_{inner}) of 12 mm in the output. It was almost the same as the 2ω beam, although only 20% of the energy is concentrated into the central peak. However, enough intensity was supplied in the experiment. The measured confocal parameter was well above 14 mm.

Helium and neon were chosen as nonlinear media because of their high ionization potentials. The gas density in the interaction volume can be varied by changing the backing pressure, but was typically controlled within 30 torr in order to reduce the defocusing effects induced by the plasma [18].

The generated harmonics were analyzed on axis by a spectrometer (Model SXR-II-1, Hettrick Scientific) consisting of a horizontal collecting toroidal mirror, a spectral focusing toroidal mirror and a choice of gratings covering different wavelength ranges. All of them were coated with gold. In order to optimize the collection efficiency, we imaged the harmonic source directly on a charge-coupled device (CCD/SX-TE, Princeton Instruments), without an entrance slit. The toroidal mirror was placed at 65 cm from the laser focus to prevent the damage by the incident laser light. The annular ω beam was blocked by an iris and the 2ω beam was eliminated by various filters. The scattered low-order harmonics and residual two-color beams were blocked by a trap to eliminate the background on the CCD.

III. RESULTS

The optimization of the spatial and temporal overlap of the two-color pulses was performed by maximizing the yield of the even-order harmonic, the 44th of the fundamental pulse. It is necessary to verify the accurate overlap in time by an auxiliary way such as the generation of 3ω by focusing the two-color pulses into a BBO crystal before they entered into the vacuum chamber. The group delay difference between ω and 2ω owing to the entrance window was taken into account.

Throughout the experiments, whether or not the two-color laser intensities are above the saturation intensities (I_s) of ionization plays a crucial role, where I_s was defined as the

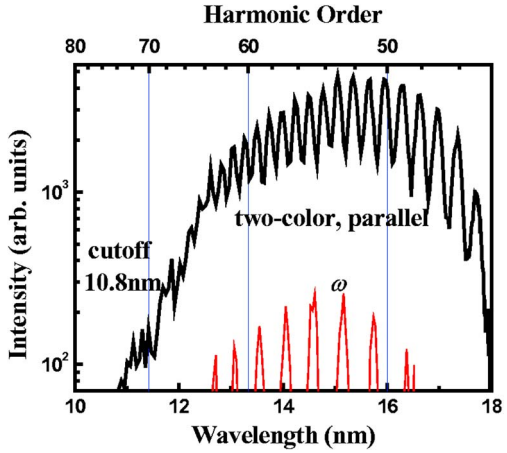

FIG. 3. (Color online) Harmonic spectra in neon observed in the two-color field (heavy solid line), ω field (light solid line) at the region of shorter wavelength. $I_\omega = 7.6 \times 10^{14}$ W/cm^2, $I_{2\omega} = 1.2 \times 10^{15}$ W/cm^2, and $r = E_{2\omega}/E_\omega = 1.3$. The spectrum by 2ω is not observed in this region.

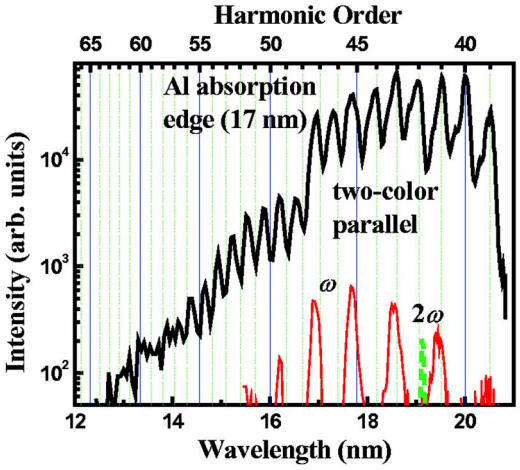

FIG. 4. (Color online) Harmonic spectra in neon observed in the two-color field (heavy solid line), ω field (light solid line), and 2ω field (dashed line) at the longer wavelength region. $I_\omega = 6.9 \times 10^{14}$ W/cm^2, $I_{2\omega} = 1.2 \times 10^{15}$ W/cm^2, and $r = E_{2\omega}/E_\omega = 1.3$.

intensity when 98% of neutral atoms are ionized. Assuming Ammosov-Delone-Krainov (ADK) ionization rates [19], and taking into account the different pulse widths of the two-color beams [20,21], we obtained $I_s = 1.1 \times 10^{15}$ W/cm^2 for ω and $I_s = 1.3 \times 10^{15}$ W/cm^2 for 2ω in neon, $I_s = 2.3 \times 10^{15}$ W/cm^2 for ω and $I_s = 2.7 \times 10^{15}$ W/cm^2 for 2ω in helium. The ionization in the two-color field was numerically calculated as parameters of the field ratio ($r = E_{2\omega}/E_\omega$) and relative phase Φ for the individual case.

A. Efficient higher-order harmonic generation in the ω-2ω field

According to the picture of three-step model, the cutoff law for the energy of the highest harmonics is predicted to be $I_p + 3.17U_p$, where I_p is the ionization potential of the atoms, $U_p = 9.33 \times 10^{-14} I$ (W cm^{-2}) λ^2 (μm) in electron volts denotes the ponderomotive potential of the laser field. For long pulses, the maximum value of U_p is limited by the intensity determined with dc tunneling theory. However, atoms can survive to higher laser intensities before being ionized if ultrashort pulses are employed [21,22]. Then the electron would be exposed to a stronger, rapidly increasing laser field before the reencountering its parent ion. This results in the generation of more intense and higher-energy harmonic radiation. The pulse duration of 2ω (24 fs) was shorter than that of ω (40 fs) in our experiment, then we can control the ionization process on the steep rise of the two-color pulse near the peak by choosing the appropriate condition in which the peak intensities of ω and 2ω pulses are less than the saturation intensity (I_s) while the intensity of the combined field is above I_s.

After confirming the perfect overlap of the two-color pulses in time and space, and choosing appropriate peak intensities of ω and 2ω pulses, a harmonic spectrum in neon was obtained as shown in Fig. 3, as well as the spectra obtained using ω field alone. It should be emphasized that all of the spectra in this paper are thought to be phase averaged since the exposure time of the CCD was usually set longer than 1 s. A 0.3$-\mu$m thick zirconium (Zr) filter was used to block the stray laser light, and a 50-cm focal-length concave mirror was utilized in this case. The peak intensities of ω and 2ω pulses were measured to be 7.6×10^{14} W/cm^2 and 1.2×10^{15} W/cm^2, and the corresponding field ratio was 1.3. The falloff in the spectra towards long wavelength is a synthetic result of the sensitivity of the spectrometer with the detector and the transmission of the Zr filter. In the case of two-color field, even-order harmonics had comparable intensities as odd harmonics. This is due to the breaking of inversion symmetry in the optical field, as mentioned above. Compared to the harmonics generated by the fundamental field alone, the two-color harmonics were enhanced by a factor of more than 10. Moreover, the cutoff of the harmonic plateau in the two-color field extended to 10.8 nm, while those were 12.7 nm and 19 nm respectively in the cases of using the ω or 2ω field alone.

A dramatic enhancement of the two-color harmonics in the longer wavelength region was observed as shown in Fig. 4. The enhancement ratio was larger than 250, comparing the 41st harmonic generated by the two-color field with that by the fundamental field alone. At the 42nd harmonic, the enhancement ratio was more than 270 compared with the 2ω field alone. A drop of harmonic radiation at 17 nm is due to the absorption edge of an aluminum filter, which was used to reduce the background noise on the CCD. Since the transmission of the 0.15-μm thick Al filter was higher than that of a Zr filter and the CCD will saturate, we moderately decreased the peak intensities of ω and 2ω pulses to 6.9×10^{14} W/cm^2 and 1.2×10^{15} W/cm^2 with $r = 1.3$. It is clear that at the longer wavelength region, a much higher conversion efficiency of two-color harmonic generation can be obtained than at the shorter wavelength region.

Similar spectrum was observed in helium as shown in Fig. 5. Because helium has the highest ionization potential among the rare gases, higher-order harmonics should be generated in helium than in neon when the intensities of the two-color pulses were properly increased at the same time. In this case,

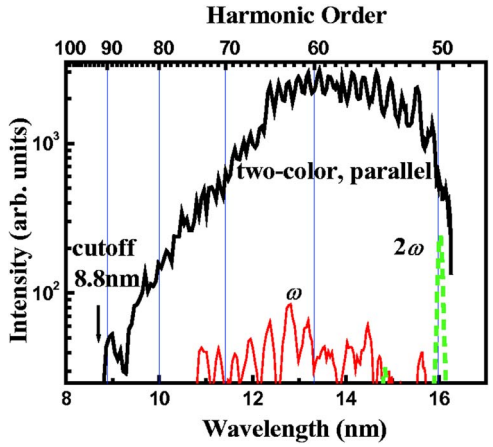

FIG. 5. (Color online) Harmonic spectra in helium observed in the two-color field (heavy solid line), ω field (light solid line), and 2ω field (dashed line). $I_\omega = 9.3 \times 10^{14}$ W/cm^2, $I_{2\omega} = 1.8 \times 10^{15}$ W/cm^2, and $r = E_{2\omega}/E_\omega = 1.4$.

the peak intensities of ω and 2ω pulses were 9.3×10^{14} W/cm^2 and 1.8×10^{15} W/cm^2 with $r = 1.4$. The cutoffs of the harmonic plateau were 8.8 nm for the ω-2ω field, 10.5 nm for the ω field, and 14.8 nm for the 2ω field respectively. The harmonic intensities were stronger than those obtained in the ω field by a factor of more than 30 at the 13-nm region.

The original concave mirror was replaced by a 100-cm focal-length concave mirror to obtain a longer confocal parameter. A significant extension of two-color harmonic cutoff order up to 111th, which corresponded to a wavelength of 7.2 nm, was observed in helium when we increased the peak intensities of the ω and 2ω fields up to 1.1×10^{15} W/cm^2 and 2.0×10^{15} W/cm^2 respectively, as shown in Fig. 6. The corresponding field ratio was 1.3. The shortest wavelength of harmonic generation in the two-color field was much shorter than the cutoff by using the ω (83rd, 9.6 nm) or 2ω field (54th, 14.8 nm) alone. The harmonic intensities were enhanced more than those generated in the single field (ω or 2ω field) by a factor of more than 10.

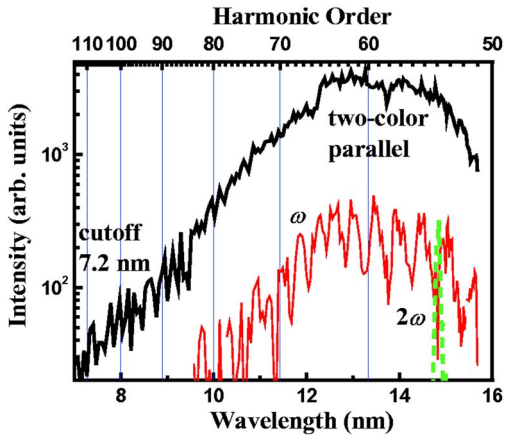

FIG. 6. (Color online) Harmonic spectra in helium observed in the two-color field (heavy solid line), ω field (light solid line), and 2ω field (dashed line). $I_\omega = 1.1 \times 10^{15}$ W/cm^2, $I_{2\omega} = 2.0 \times 10^{15}$ W/cm^2, and $r = E_{2\omega}/E_\omega = 1.3$.

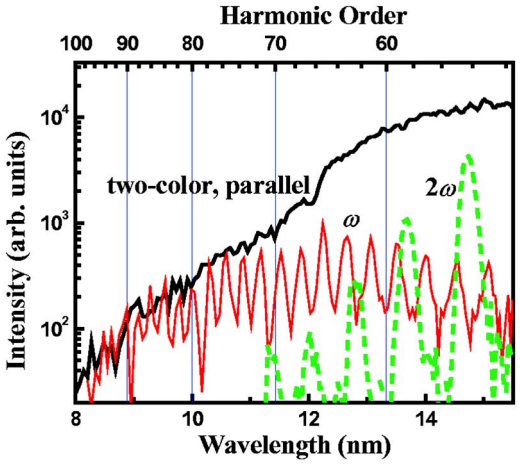

FIG. 7. (Color online) Harmonic spectra observed in helium where the intensities of ω and 2ω pulses are near or larger than the saturation intensities. $I_\omega = 2.0 \times 10^{15}$ W/cm^2, $I_{2\omega} = 2.9 \times 10^{15}$ W/cm^2, and $r = E_{2\omega}/E_\omega = 1.2$.

In the preceding experiments, the intensities of the ω and 2ω fields were set well below the saturation intensities. However, the significant features of the enhancement and the extension of the cutoff decrease or disappear when the intensities of the ω and 2ω fields are near or above the saturation intensities. The cutoff of the two-color harmonic plateau was not extended any more when the peak intensities of ω and 2ω pulses were increased up to 2.0×10^{15} W/cm^2 and 2.9×10^{15} W/cm^2 respectively, as shown in Fig. 7. The harmonic intensity in the two-color field was almost the same as that in the fundamental field below 10 nm. Harmonics are generated progressively from the lower to higher order in the leading edge of the driving pulse and the cutoff is determined by the saturation intensity of ionization. Then the relatively low-order harmonics, which saturate in the low intensity, are enhanced by the two-color field. However, the intensities of the high orders are limited by ionization with the single field and the two-color field does not work.

As the intensities of the ω and 2ω fields increase from Fig. 5 to Fig. 7, the modulation of the spectrum by individual harmonic disappears, leading to the supercontinuum in Fig. 7. This may not be due to a wash-out effect coming from the varying carrier envelope phase of the pulses [23] because the pulses used in this experiment contain 15 cycles and also because the transition to the supercontinuum depends on the intensity of the ω-2ω field. This can be explained by the self-phase modulation of the excitation pulses and then of the harmonics which induces a significant blue shift of harmonics [24]. Even though a multilayer mirror (Mo/Si) with the highest reflectance is available in this region, the supercontinuum near 10 nm is only a necessary but not sufficient condition for the generation of attosecond pulses. The phase should be flat over the entire bandwidth. However, this is another issue to be solved. In this experiment the phase may not be flat because of the self-phase modulation.

B. Polarization dependence of two-color harmonics

To change the polarization of the beam, a half-wave plate for 800 nm was inserted in the ω path, as mentioned above.

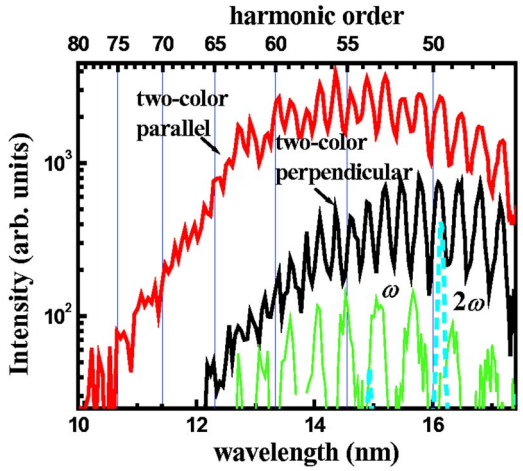

FIG. 8. (Color online) Polarization-dependent harmonic spectra in helium observed in the two-color field (heavy solid line) as well as in the monochromatic field (light solid line for the ω field and dashed line for the 2ω field). $I_\omega = 8.0 \times 10^{14}$ W/cm^2, $I_{2\omega} = 1.9 \times 10^{15}$ W/cm^2, and $r = E_{2\omega}/E_\omega = 1.5$.

The grating in the spectrometer was insensitive to polarization since there was no substantial change of harmonic intensities generated by the ω beam with different polarizations. Polarization-dependent harmonic spectra in helium are shown in Fig. 8. The peak intensities of the ω and 2ω fields were measured to be 8.0×10^{14} W/cm^2 and 1.9×10^{15} W/cm^2, with $r = 1.5$. It is clear that more intense higher-order harmonics were obtained in the parallel two-color field than in the perpendicular two-color field. However, even in the perpendicular field, even-order harmonics had comparable intensities as odd harmonics in addition to the enhancement of harmonics, which are different from the results of other groups [5,9], where the even harmonics were much weaker than the odd ones. The imperfect polarization direction of the beams in this experiment may account for the observation.

We have not observed the enhancement in the orthogonally polarized two-color field beyond the parallel polarized two-color field, which was observed around 20 nm in Ref. [10]. We think that this observation in Ref. [10] may be possible in the special condition with phase control where the electrons return to the core. However, in the shorter wavelength, the parallel polarized two-color field will always give us the stronger harmonics.

IV. ANALYSIS

The cutoff energy in the monochromatic field is expressed as $I_p + \alpha U_p$ ($\alpha = 3.17$) by the three-step model. This relation corresponds to the cutoff of the square of atomic dipole moments. However, in the real experiments, the observed spectrum results from the phase matching term in addition to the single atom response and the effective value of α_e is around 2 [25]. The experimental cutoff was determined by the highest order observed in the dynamic range of the experiment although it contains some uncertainty. The values of α_e were 1.6 to 1.8 from Figs. 3–6 in the ω field while they were 2.0 to 2.5 in the 2ω field. The difference of α_e in the two fields would come from the difference in phase-matching length between the Bessel-Gauss and Gauss beam and from the difference in the pulse duration.

In the monochromatic field, there are two trajectories: long and short trajectories for the given kinetic energy of returning electrons. Usually the contribution of the long trajectory to a spectrum is neglected because of the spread of the wave function. This behavior has a periodicity of every half cycle as well as in the ω-3ω field. However, in the ω-2ω field, this periodicity is broken and there may be many trajectories for a given kinetic energy, resulting in a splitting of the cutoff into two branches, an upper and a lower branch [26].

The harmonic spectrum in the ω-2ω field is interpreted intuitively by the classical analysis. The combined field is expressed as

$$E(t) = E_\omega \sin(\omega t) + E_{2\omega} \sin(2\omega t + \Phi). \tag{1}$$

According to the three-step model, the electron tunneling into the continuum at time t_0 with the initial conditions of $\mathbf{r}(t_0) = 0$ and $\mathbf{v}(t_0) = 0$, where $\mathbf{r}(t)$ and $\mathbf{v}(t)$ are the position and velocity of the electron. Then it returns at time t_1 with $\mathbf{r}(t_1) = 0$, i.e., reencounters at the position of its parent ion. Hence the classical trajectories of the electron can be obtained from the Newton's equation:

$$\begin{aligned}\mathbf{r}(t_1) = {} & (E_\omega/\omega^2)[-\sin(\omega t_0) + \sin(\omega t_1) - \omega(t_1 - t_0)\cos(\omega t_0)] \\ & + (E_{2\omega}/4\omega^2)[-\sin(2\omega t_0 + \Phi) + \sin(2\omega t_1 + \Phi) \\ & - 2\omega(t_1 - t_0)\cos(2\omega t_0 + \Phi)].\end{aligned} \tag{2}$$

Assuming excursion time $\tau = t_1 - t_0$ is the time the electron spent in the continuum, and restricting $0 < t_0 < T, 0 < \tau < T$, where T is the optical cycle of ω. The kinetic energy obtained by the electron from the laser field while in the continuum is expressed as $E_{kin}(t_1, t_0) = 0.5 \times [A(t_1) - A(t_0)]^2$, where $A(t)$ is the vector potential and $E(t) = -\partial A(t)/\partial t$. Then the harmonic cutoff is given by $I_p + E_{max}$, where E_{max} is the maximum kinetic energy of the electron.

Defining the ponderomotive energy as $U_p = (E_\omega^2/4\omega^2) + (E_{2\omega}^2/16\omega^2)$, t_0 and t_1 were calculated as a function of the kinetic energy, as shown in Fig. 9. The parameters were chosen as $I_\omega = 9.0 \times 10^{14}$ W/cm^2, $I_{2\omega} = 1.5 \times 10^{15}$ W/cm^2, $r = 1.3$, and $\Phi = 0$ (a) or $\Phi = 0.5\pi$ (b), where the peak of the two-color field almost corresponds the saturation of ionization. Figure 10 shows the corresponding instantaneous two-color electric field at the same conditions. It is clear that the cutoff energy splits into two branches [26], where the corresponding emission times were marked as t_{upper} and t_{lower} in Fig. 9. It should be noted that there still is the third branch in Fig. 9, whose emission time was marked as t_{ignore}. The contributions from this branch can be ignored because the electric field at the emission time of t_{ignore} is very weak, as shown in Fig. 10. Then the electrons cannot tunnel from the ground state at that time. The upper and the lower cutoff branches have comparable excursion times. However, the electric field at the emission time of t_{lower} is much larger than that at t_{upper} as shown in Fig. 10. This situation is true at 0

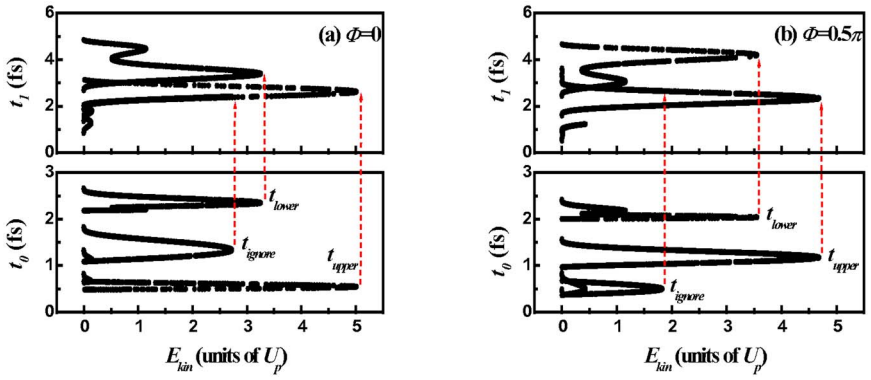

FIG. 9. (Color online) Classical emission time (t_0) and return time (t_1) as a function of the kinetic energy E_{kin} for $I_\omega = 9.0 \times 10^{14}$ W/cm^2, $I_{2\omega} = 1.5 \times 10^{15}$ W/cm^2, $r = 1.3$, and $\Phi = 0$ (a) or $\Phi = 0.5\pi$ (b) where the saturation of ionization occurs in the two-color field.

$\leq \Phi \leq 0.7\pi$. The phase-averaged two-color field from the lower branch is larger by a factor of 2.05 than that of the ω field. Therefore, the harmonic intensity at the lower branch is larger than those of the ω field [4] and of the upper branch [26] by many orders of magnitude.

The observed phase-averaged higher intensities of two-color harmonics in the longer wavelength region are obviously due to the lower branch. The values of α for the lower branch excluding the phase-matching effect vary between 2.3 and 4.3 depending on phase. The phase-averaged value of α is up to 3.3 when U_p is $(E_m^2/4\omega^2)+(E_{2\omega}^2/16\omega^2)$. The effective values of α_e including the phase-matching effect are 1.6 to 2.1 from Figs. 3–6. These values are almost equal to those in the ω or 2ω field alone, indicating the similar phase-matching condition. Therefore, the observed extension of the cutoff is partly explained by the increase of U_p in the two-color field. Another possible reason is that the cutoff looks to be extended in the used dynamic range from the enhanced intensity. The contribution of the upper branch would not apply in this case because the harmonic intensity is much lower than that of the lower branch.

However, once the peak intensities of the ω and 2ω fields are increased larger than the saturation intensities, the notable ionization would destroy the enhancement because the generation of two-color harmonics ceases with the ionization of neutral atoms. Hence, the harmonics from the upper branch are difficult to be observed experimentally, which restricts the extension of two-color harmonic plateau to the region of the water window.

V. DISCUSSION

Important parameters for the enhancement of harmonic generation in the two-color field are the intensities and the field ratio of the ω and 2ω pulses, which can be observed from Figs. 3–8. The higher the field ratio is, the more significant enhancement one can obtain, which accords with the conclusions of other reports [3,4,11,26,27]. However, the field ratio cannot be increased infinitely due to the intensity of the combined field restricted by the saturation intensity. Increasing the intensity of the 2ω field means decreasing the weight of the ω field correspondingly, which induces the reduction of U_p and therefore shortens the plateau. Choosing comparable intensities of the ω and 2ω fields one can make a compromise between the harmonic enhancement and the extension of cutoff frequency.

What we found in this experiment, compared with the previous works [3–5,8–10], are (1) the significant enhancement of harmonics below 17 nm, (2) the extension of the cutoff down to 7 nm, and (3) the generation of the supercontinuum below 13 nm. We think they were realized by the short 2ω pulse width used, along with the sufficient 2ω intensity, which was generated by broadband frequency doubling (BFD). However, BFD prevents the control of the relative phase between the ω and 2ω fields because the optical path of BFD is too long. Obviously, the phase-averaged spectra impeded the further extension of the cutoff.

The atomic dipole moment calculated by the strong field approximation in Ref. [4] shows the two-step structure in the cutoff region; the cutoff of the low-order step corresponds to that of the ω field alone but the intensity is enhanced, and the cutoff of the higher-order step is extended but the intensity is less than that of the ω field alone. This two-step structure corresponds to two electron trajectories and is clearly assigned as the lower and upper branches [26].

The experimental fact that the enhancement is significant but the extension of the cutoff is less than expected is attributed to the contribution of the lower branch but not the upper

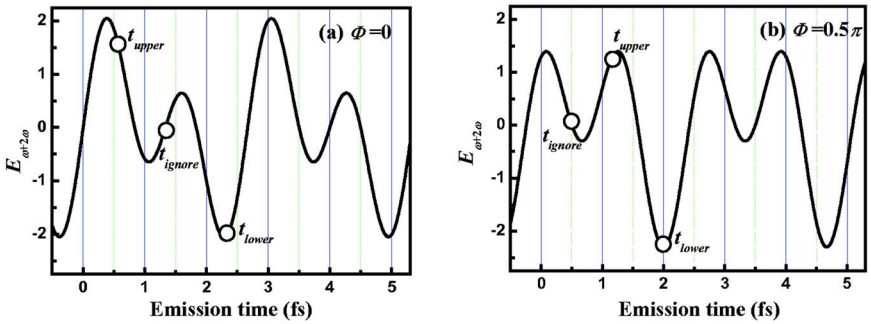

FIG. 10. (Color online) Instantaneous two-color electric field for $r = 1.3$ and $\Phi = 0$ (a) or $\Phi = 0.5\pi$ (b). The amplitude of E_ω was assumed to be 1.

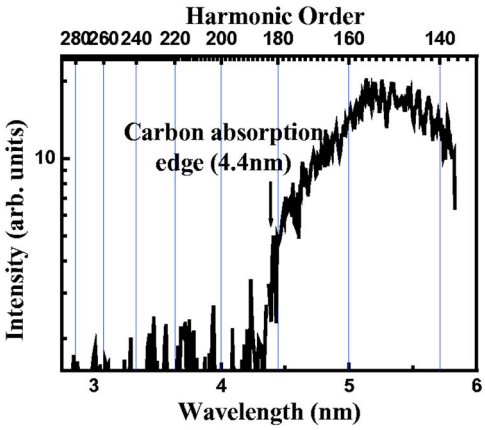

FIG. 11. (Color online) Harmonic spectrum in helium observed using circular ω beam. $I_\omega = 7 \times 10^{15}$ W/cm^2. The absorption edge of parylene filter at 4.4 nm verified that the generated harmonics achieved in the region of the water window.

branch. This is quite informative to this research field because one cannot expect the contribution of the upper branch in the real experiment.

We used an annular ω beam to eliminate the dispersion of beam splitters. This degraded the phase matching compared with the circular 2ω beam because the effective values of α_e were a little less than those of 2ω. We also tried the harmonic generation of the water window in the nonadiabatic regime [1,2] using circular ω beam alone, as shown in Fig. 11. Two pieces of 0.2-μm thick parylene filters were used to calibrate the wavelength. The absorption edge at 4.4 nm confirmed the harmonic generation achieved in the region of the water window. However, the peak intensity was measured up to 7×10^{15} W/cm^2 at that time, which was much higher than the saturation intensity. The harmonic intensity in the water window was quite low compared with Figs. 3–8. Then the extension of the cutoff in the two-color field is one of the ways to the intense harmonics in the water window.

The most efficient way to the enhanced harmonic generation in the water window is the phase control between the ω and 2ω field. When $\Phi = 0.7\pi$, α increased to 4.3 instead of $\alpha = 3.3$ in the phase-average condition. However, BFD did not enable us to control the phase owing to the disturbance in air and vibration of a table during the long optical path. The simple addition of a thin BBO crystal would broaden the pulse width by the group-velocity mismatch (150 fs/mm) although the phase control would be possible [10]. The phase control with a sufficiently short pulse and enough energy at 2ω obviously needs a new system. The further pulse shortening of the ω and 2ω fields would help the extension of the cutoff because of the increase in saturation intensity of ionization. Actually, we tried it by 27-fs ω pulses and 17-fs 2ω pulses, but the cutoff could not be extended. Although 16-fs ω pulses and 8-fs 2ω pulses were obtained in a 1–5 KHz system [16], the intensities of the ω and 2ω fields are not sufficient for this experiment.

VI. CONCLUSION

Using a linearly polarized ω-2ω field we observed efficient high-order harmonic generation in neon and helium. Even-order harmonics with intensities comparable to odd harmonics were generated from the asymmetry electric field. The enhancement due to the two-color field compared to the ω or 2ω field alone was by more than one order of magnitude. The cutoff was extended to 7.2 nm. These phenomena were explained by the contribution of the lower branch rather than the upper branch, which are split in the ω-2ω field. The efficient soft x-ray continuum near 10 nm provides the bandwidth capable of attosecond pulses although the phase should be controlled at the same time. The intense harmonics in the water window are expected by using the two-color field with a fixed relative phase and much shorter pulse durations.

[1] E. Seres, J. Seres, F. Krausz, and C. Spielmann, Phys. Rev. Lett. **92**, 163002 (2004).
[2] E. A. Gibson, A. Paul, N. Wagner, R. Tobey, D. Gaudiosi, S. Backus, I. P. Christov, A. Aquila, E. M. Gullikson, D. T. Attwood, M. M. Murnane, and H. C. Kapteyn, Science **302**, 95 (2003).
[3] S. Watanabe, K. Kondo, Y. Nabekawa, A. Sagisaka, and Y. Kobayashi, Phys. Rev. Lett. **73**, 2692 (1994).
[4] K. Kondo, Y. Kobayashi, A. Sagisaka, Y. Nabekawa, and S. Watanabe, J. Opt. Soc. Am. B **13**, 424 (1996).
[5] H. Eichmann, A. Egbert, S. Nolte, C. Momma, B. Wellegehausen, W. Becker, S. Long, and J. K. McIver, Phys. Rev. A **51**, R3414 (1995).
[6] P. B. Corkum, Phys. Rev. Lett. **71**, 1994 (1993).
[7] M. B. Gaarde, A. L'Huillier, and M. Lewenstein, Phys. Rev. A **54**, 4236 (1996).
[8] U. Andiel, G. D. Tsakiris, E. Cormier, and K. Witte, Europhys. Lett. **47**, 42 (1999).
[9] M. D. Perry and J. K. Crane, Phys. Rev. A **48**, R4051 (1993).
[10] I. J. Kim, C. M. Kim, H. T. Kim, G. H. Lee, Y. S. Lee, J. Y. Park, D. J. Cho, and C. H. Nam, Phys. Rev. Lett. **94**, 243901 (2005).
[11] D. B. Milošević and W. Sandner, Opt. Lett. **25**, 1532 (2000); D. B. Milošević, W. Becker, and R. Kopold, Phys. Rev. A **61**, 063403 (2000).
[12] X. M. Tong and Shih-I Chu, Phys. Rev. A **58**, R2656 (1998).
[13] T. Sekikawa, A. Kosuge, T. Kanai, and S. Watanabe, Nature **432**, 605 (2004).
[14] R. Kienberger, E. Goulielmakis, M. Uiberacker, A. Baltuska, V. Yakovlev, F. Bammer, A. Scrinzi, Th. Westerwalbesloh, U. Kleineberg, U. Heinzmann, M. Drescher, and F. Krausz, Nature **427**, 817 (2004).
[15] J. Itatani, Y. Nabekawa, K. Kondo, and S. Watanabe, Opt. Commun. **134**, 134 (1997).
[16] T. Kanai, X. Y. Zhou, T. T. Liu, A. Kosuge, T. Sekikawa, and S. Watanabe, Opt. Lett. **29**, 2929 (2004); T. Kanai, X. Y. Zhou, T. Sekikawa, S. Watanabe, and T. Togashi, Opt. Lett. **28**, 1484 (2003).

[17] C. Altucci, R. Bruzzese, D. D'Antuoni, C. de Lisio, and S. Solimeno, J. Opt. Soc. Am. B **17**, 34 (2000); C. F. R. Caron and R. M. Potvliege, J. Opt. Soc. Am. B **15**, 1096 (1998).
[18] T. Adachi, K. Kondo, and S. Watanabe, Appl. Phys. B **55**, 323 (1992).
[19] M. V. Ammosov, N. B. Delone, and V. P. Krainov, Sov. Phys. JETP **64**, 1191 (1986).
[20] B. Chang, P. R. Bolton, and D. N. Fittinghoff, Phys. Rev. A **47**, 4193 (1993).
[21] Z. H. Chang, A. Rundquist, H. W. Wang, M. M. Murnane, and H. C. Kapteyn, Phys. Rev. Lett. **79**, 2967 (1997).
[22] I. P. Christov, J. Zhou, J. Peatross, A. Rundquist, M. M. Murnane, and H. C. Kapteyn, Phys. Rev. Lett. **77**, 1743 (1996).
[23] A. Baltuška, M. Uiberacker, E. Goulielmakis, R. Kienberger, V. S. Yakovlev, T. Udem, T. W. Hänsch, and F. Krausz, IEEE J. Sel. Top. Quantum Electron. **9**, 972 (2003).
[24] T. Sekikawa, T. Kumazaki, Y. Kobayashi, Y. Nabekawa, and S. Watanabe, J. Opt. Soc. Am. B **15**, 1406 (1998).
[25] C. G. Wahlström, J. Larsson, A. Persson, T. Starczewski, S. Svanberg, P. Salières, P. Balcou, and A. L'Huillier, Phys. Rev. A **48**, 4709 (1993); A. L'Huillier, M. Lewenstein, P. Salières, Ph. Balcou, M. Yu. Ivanov, J. Larsson, and C. G. Wahlström, Phys. Rev. A **48**, R3433 (1993).
[26] C. Figueira de Morisson Faria, D. B. Milošević, and G. G. Paulus, Phys. Rev. A **61**, 063415 (2000); C. F. de Morisson Faria, M. Dörr, W. Becker, and W. Sandner, Phys. Rev. A **60**, 1377 (1999).
[27] M. Protopapas, A. Sanpera, P. L. Knight, and K. Burnett, Phys. Rev. A **52**, R2527 (1995).